NANO LETTERS

Letter

pubs.acs.org/NanoLett

Enhanced Ferroelectric-Nanocrystal-Based Hybrid Photocatalysis by Ultrasonic-Wave-Generated Piezophototronic Effect

Haidong Li,[†,⊥] Yuanhua Sang,[†,⊥] Sujie Chang,[†] Xin Huang,[‡] Yan Zhang,[‡] Rusen Yang,[§] Huaidong Jiang,[†] Hong Liu,*[,†,‡] and Zhong Lin Wang*[,‡,∥]

[†]State Key Laboratory of Crystal Materials, Shandong University, Jinan 250100, China

[‡]Beijing Institute of Nanoenergy and Nanosystems, Chinese Academy of Sciences, Beijing 100083, China

[§]Department of Mechanical Engineering, University of Minnesota, Minneapolis, Minnesota 55455, United States

[∥]School of Material Science and Engineering, Georgia Institute of Technology, Atlanta, Georgia 30332−0245, United States

Supporting Information

ABSTRACT: An electric field built inside a crystal was proposed to enhance photoinduced carrier separation for improving photocatalytic property of semiconductor photocatalysts. However, a static built-in electric field can easily be saturated by the free carriers due to electrostatic screening, and the enhancement of photocatalysis, thus, is halted. To overcome this problem, here, we propose sonophotocatalysis based on a new hybrid photocatalyst, which combines ferroelectric nanocrystals ($BaTiO_3$) and semiconductor nanoparticles (Ag_2O) to form an Ag_2O−$BaTiO_3$ hybrid photocatalyst. Under periodic ultrasonic excitation, a spontaneous polarization potential of $BaTiO_3$ nanocrystals in responding to ultrasonic wave can act as alternating built-in electric field to separate photoinduced carriers incessantly, which can significantly enhance the photocatalytic activity and cyclic performance of the Ag_2O−$BaTiO_3$ hybrid structure. The piezoelectric effect combined with photoelectric conversion realizes an ultrasonic-wave-driven piezophototronic process in the hybrid photocatalyst, which is the fundamental of sonophotocatalysis.

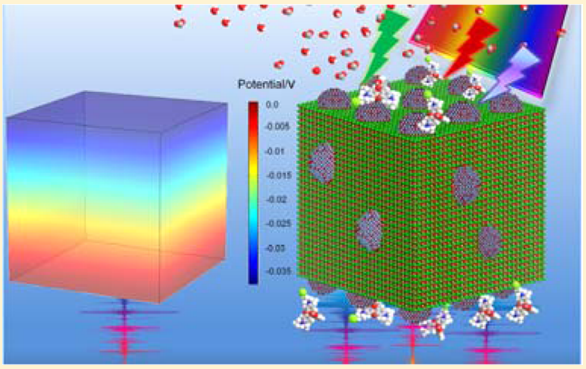

KEYWORDS: *built-in electric field, ultrasonic wave, sonophotocatalysis, piezophototronics*

One of the most important problems for prohibiting industrial applications of photocatalysis is low photocatalytic activity caused by photoinduced carrier recombination in semiconductor photocatalyst, which causes neutralization of the photoinduced electrons and holes before they can initiate the photocatalytic processes.[1−7] Although some measures based on heterostructures have been proposed and put into practice to solve this problem, the efficiency is still too low to separate electron−hole pairs completely during photocatalysis.[2,3,7−17] Recently, a new concept, introducing a built-in electric field (internal field) in photocatalyst particles,[14,18−25] was proposed to enhance the separation of photoinduced charge carriers. The presence of the built-in electric field provides a driving force for the transport of photoinduced charge carrier, thus enhancing their separation.[1,2,24−26] Although the built-in electric field can separate photoinduced carriers, a static field can be easily saturated by free carries, and the enhancement of the photocatalysis, thus, is halted.[2,25] Renewing built-in electric field and keeping the photoinduced carrier separation incessantly during photocatalysis process is the greatest challenge for keeping high performance of photocatalyst with a built-in electric field.

Ferroelectrics with an intrinsic built-in electric field have not been utilized to enhance photocatalytic property simply by combing them with metal-oxide-semiconductor materials. As is well known, ferroelectric crystal possesses spontaneous polarization potential, and the potential can be altered by applying a stress to the crystal owing to piezoelectricity.[27−32] As reported, the piezopotential can effectively influence charge transport resulting in significantly enhanced optoelectronic performances. This is known as the piezophototronic effect presence in piezoelectric-semiconductor materials.[33−41] Different from the built-in fields in other nanoparticles, the internal potential of nanoferroelectrics can be alternately enlarged and diminished by applying stress driven by mechanical vibration or ultrasonic waves.[33,35−37,40,42] Several studies have proposed the concept that ultrasonic wave can be used as irradiation energy source[43−51] to enhance photocatalysis and realize sonocatalysis.[50,52−57] The sonophotocatalytic treatment for chemical reaction and pollution degradation were proposed and discussed.[58−60] The enhanced catalytic property was attributed

Received: December 2, 2014
Revised: March 22, 2015

DOI: 10.1021/nl504630j
Nano Lett. XXXX, XXX, XXX−XXX

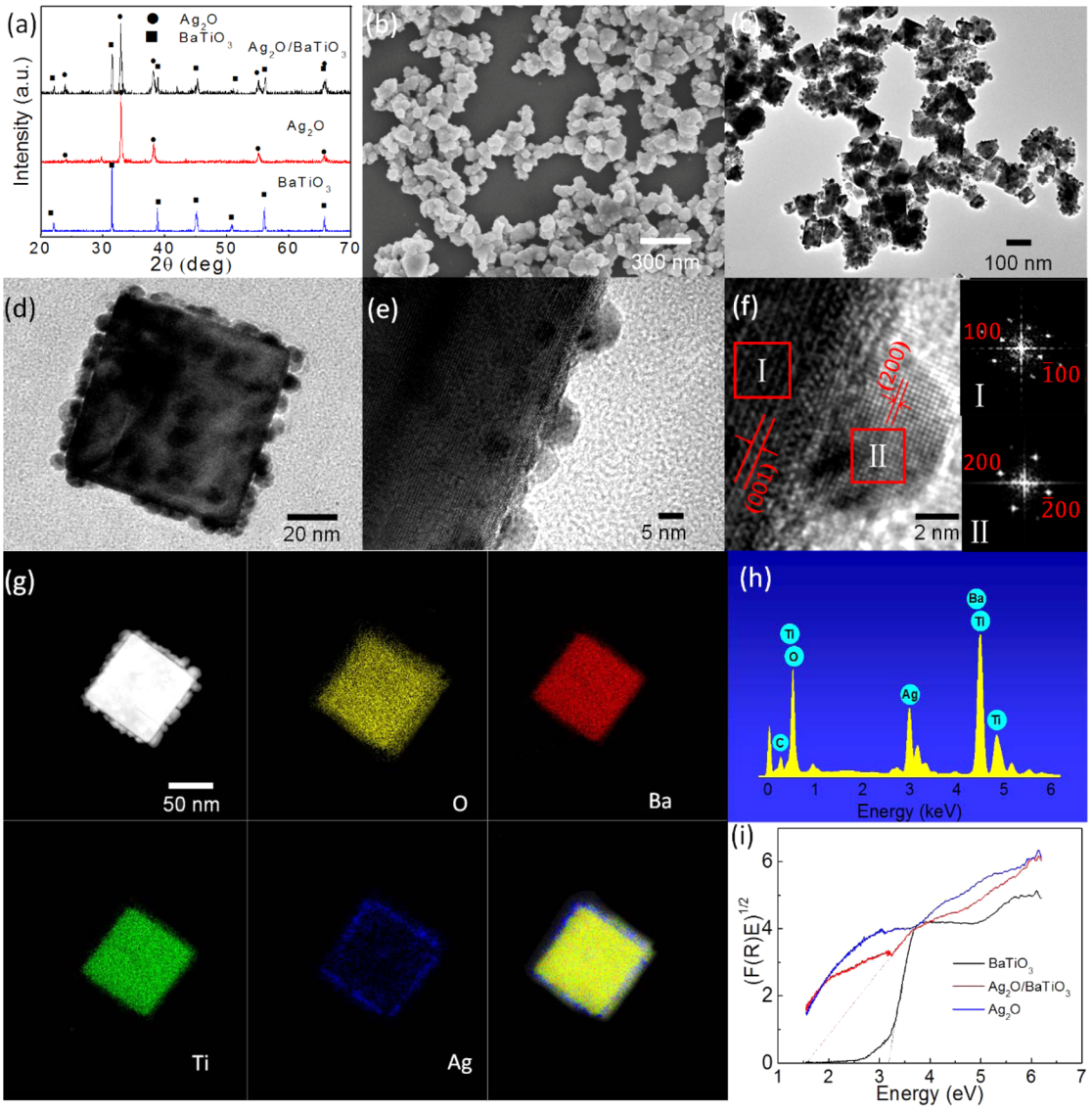

Figure 1. Structure of Ag_2O−$BaTiO_3$ hybrid photocatalyst. (a) XRD patterns of the as-synthesized products: Ag_2O particles, $BaTiO_3$ nanocubes and Ag_2O−$BaTiO_3$ hybrid nanocubes (20:10); (b) SEM images of Ag_2O−$BaTiO_3$ hybrid nanocubes; (c, d, e) TEM images of Ag_2O−$BaTiO_3$ nanocubes (20:10) with different magnification; (f) HRTEM image of Ag_2O−$BaTiO_3$ nanocubes and fast Fourier transform pattern of Ag_2O and $BaTiO_3$; (g, h) STEM image, EDS mapping, and EDS results from Ag_2O−$BaTiO_3$ hybrid nanocubes; (i) plots of $(F(R)E)^{0.5}$ versus Eg of Ag_2O, $BaTiO_3$, and Ag_2O−$BaTiO_3$ hybrid nanocubes.

to the particle deaggregation induced by the ultrasound wave as results of possibly increased surface area of the photocatalyst, the sonoluminescence, ultrasonic cavitation effect, and sonophotochemical and sonoelectrochemical effects. No piezoelectric effect was involved for the improvement of catalytic property. In addition, another category of catalysis related to ultrasonic wave is direct water splitting[61] and azo dye decolorization in aqueous solution[62] through vibrating (i.e., ultrasonic vibration) piezoelectric ZnO microfibers or $BaTiO_3$ microdendrites, which is only based on the piezoelectrochemical catalysis caused by stress-induced piezoelectric potential of nanomaterials. However, as a piezoelectrochemical catalyst, using ultrasonic irradiation only, the rate of the catalytic degradation is limited. Most importantly, all of these works have not combined piezoelectric effect and photocatalyst together to realize the photocatalytic activity enhancement by adjusting built-in field of the piezoelectrics−semiconductor hybrid photocatalysts.

In this paper, we propose to combine ferroelectric $BaTiO_3$ nanocrystals and photocatalyst Ag_2O to form an Ag_2O−$BaTiO_3$ hybrid photocatalyst, in which, the spontaneous polarization potential of $BaTiO_3$ nanocrystals can be used as a built-in electric field, and an ultrasonic wave can be applied as driving force to alternately alter the potential created by piezoelectric effect that can avoid the saturation of the built-in field. Therefore, the built-in electric field induced carrier separation enhancement can be preserved under ultrasonic irradiation, which can continuously enhance photocatalytic performance of Ag_2O−$BaTiO_3$ hybrid photocatalyst.

As is well known, the crystal symmetry of $BaTiO_3$ can change from cubic to tetragonal when the temperature drops below the Curie point (120 °C), and the tetragonal $BaTiO_3$ nanocubes can form a built-in electric field because of its spontaneous polarization[1,63] (Supporting Information S1). The linear correlation between the electric field intensity and the stress was simulated using COMSOL (Supporting Information S2).

DOI: 10.1021/nl504630j
Nano Lett. XXXX, XXX, XXX−XXX

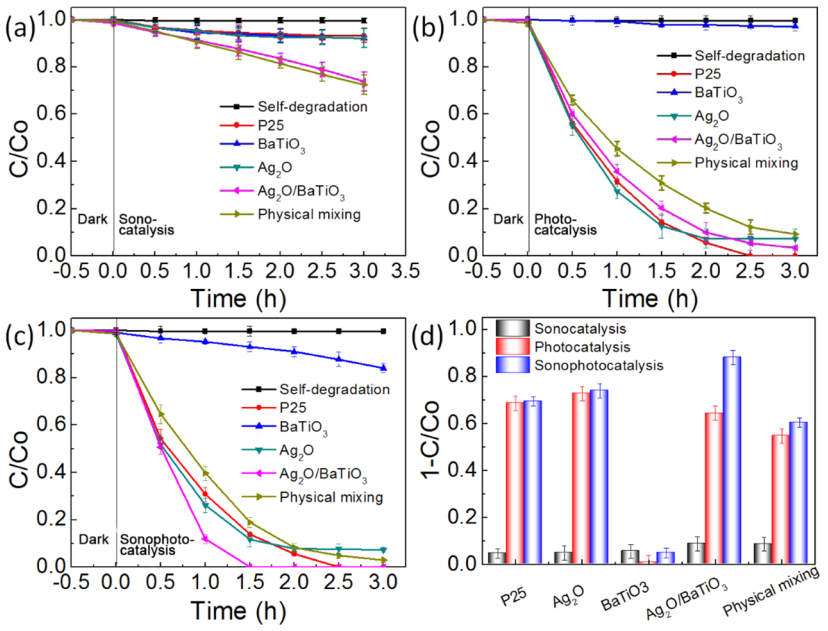

Figure 2. Degradation of Rh B as a function of irradiation time for sonocatalysis (a, under ultrasonic irradiation), photocatalysis (b, under UV light irradiation), and sonophotocatalysis (c, under both ultrasonic and UV light irradiation) in the presence of P25, Ag_2O particles, $BaTiO_3$ nanocubes, Ag_2O−$BaTiO_3$ hybrid nanocubes, physical mixture of $BaTiO_3$ and Ag_2O powder, and self-degradation without catalyst. (d) Sonocatalytic, photocatalytic, and sonophotocatalytic degradation of Rh B in the presence of P25, Ag_2O nanoparticles, $BaTiO_3$ nanocubes, Ag_2O−$BaTiO_3$ hybrid nanocubes, and physically mixed $BaTiO_3$−Ag_2O powder for 1 h.

To realize the built-in electric field enhanced photocatalysis, an efficient photocatalyst of Ag_2O was selected to be the second phase that is assembled on the $BaTiO_3$ surface to facilitate Ag_2O−$BaTiO_3$ hybrid photocatalyst. The crystal structure and morphology of $BaTiO_3$ and Ag_2O are discussed in Supporting Information S3 and S4, respectively.

In the current study, Ag_2O nanoparticles were assembled on $BaTiO_3$ nanocubes by chemical precipitation under ultrasonic irradiation. The XRD patterns (Figure 1a and Supporting Information S5) and XPS spectrum (Supporting Information S6) of the sample confirm that the Ag_2O−$BaTiO_3$ products with different weight ratios consist of tetragonal $BaTiO_3$ (PDF card no. 75-1606) and cubic Ag_2O (PDF card no. 75-1532). As shown in the SEM (Figure 1b) and TEM (Figure 1c, d, e, and f; Supporting Information S7) images, well-crystallized hemispheric Ag_2O nanoparticles with a size of 5−10 nm grow onto the surface of the $BaTiO_3$ nanocubes with preferred crystalline orientation to form the hybrid nanocubes. The interplanar distance in the Ag_2O and $BaTiO_3$ portions are ca. 0.236 and 0.403 nm (Figure 1f), corresponding to the spacing of the (200) and (001) planes of Ag_2O and $BaTiO_3$, respectively. Ag_2O nanoparticles attach on $BaTiO_3$ nanocubes tightly and cannot be detached even under long-term ultrasonic treatment (Supporting Information S8). Energy dispersive X-ray spectrometry (EDS) mapping images of an Ag_2O−$BaTiO_3$ hybrid nanocube with individual elements of Ba, Ti, O, and Ag (Figure 1g), as well the EDS spectrum (Figure 1h), further confirm that the Ag_2O nanoparticles are uniformly assembled on the surface of the $BaTiO_3$ nanocubes. The band gap of $BaTiO_3$ nanocubes and Ag_2O nanoparticles are estimated to be 3.27 and 1.3 eV,[64,65] respectively from UV−vis diffuse reflectance absorption spectra (Figure 1i and Supporting Information S9).

As expected, the built-in electric field of ferroelectric $BaTiO_3$ nanocube can enhance photocatalytic activity of Ag_2O−$BaTiO_3$ hybrid nanocube, and ultrasonic irradiation can improve the photocatalytic activity by periodically altering the built-in electric field. As is well known, the various dosage of catalyst on a cocatalyst would significantly influence the efficiency improvement. Before the intensive study of the effect of ultrasonic irradiation on the enhancement of photocatalytic property, the optimized ratio of Ag_2O−$BaTiO_3$ hybrid nanocubes in weight under 40 kHz, 50 W ultrasonic irradiation was studied first. The results imply that the optimized ratio of Ag_2O−$BaTiO_3$ hybrid nanocubes in weight is around 20:10 (Supporting Information S10). Therefore, we performed all the following experiments with Ag_2O−$BaTiO_3$ hybrid nanocube in weight ratio of 20:10.

To demonstrate the effect of ultrasonic irradiation on the photocatalytic activity of Ag_2O−$BaTiO_3$ hybrid nanocubes, the degradation capability on Rh B was evaluated under ultrasonic irradiation only, UV light only, and both ultrasonic and UV light irradiation together (Figure 2a, b, and c). For comparison, the photodegradation ability of other four samples, commercial P25 nanoparticles (anatase 80%, rutile 20%, Degussa Co. Ltd., Germany), $BaTiO_3$ nanocubes, Ag_2O nanoparticles, and a physical mixture of $BaTiO_3$ and Ag_2O were also evaluated at the same experimental condition. The results (Figure 2a) show that no degradation of Rh B can be detected by individually using P25, $BaTiO_3$ nanocubes, or Ag_2O nanoparticles as the catalyst under ultrasonic irradiation in dark. However, both the physical mixture of Ag_2O and $BaTiO_3$ and the Ag_2O−$BaTiO_3$ hybrid nanocubes induce a slight degradation of Rh B. This result illustrates that the coexistence of $BaTiO_3$ and Ag_2O is a necessary and sufficient condition for sonocatalysis. Moreover, the particle concentrations of the Ag_2O, $BaTiO_3$, and Ag_2O−$BaTiO_3$ hybrid nanocubes are different. In order to make a comparable, we performed some experiments (Supporting Information S10). The sonocatalysis of Ag_2O−$BaTiO_3$ hybrid nanocubes can be discussed by an electrocatalysis mechanism. As discussed in Supporting Information S11, when ferroelectric

DOI: 10.1021/nl504630j
Nano Lett. XXXX, XXX, XXX−XXX

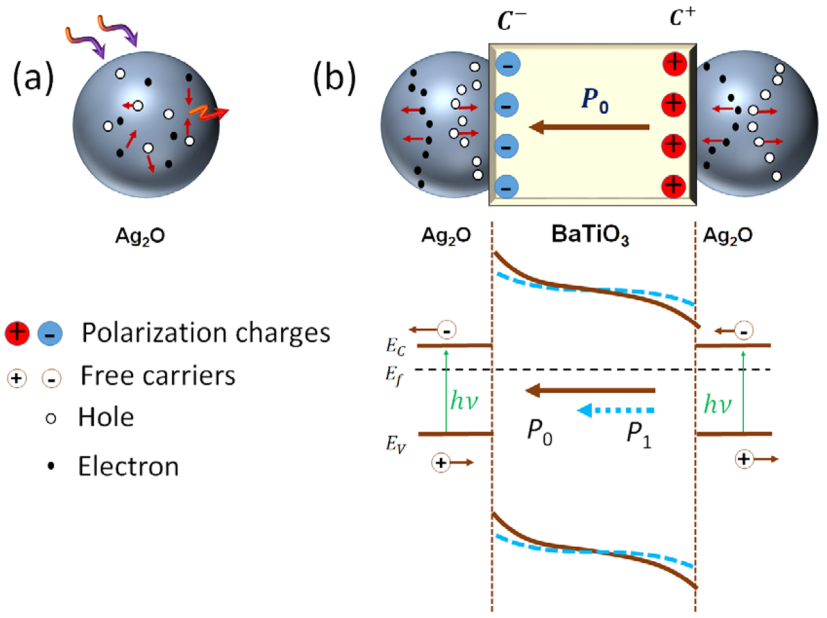

Figure 3. Schematic illustration of (a) charge carrier generation in a Ag_2O nanoparticle when excited by a photon. (b) The separation of electrons and holes in Ag_2O nanoparticles attached to the two opposite surfaces of a $BaTiO_3$ nanocube that have opposite polarization charges due to piezoelectric effect and the corresponding tilting in the bands. The solid line is the bands with the presence of spontaneous polarization charges at the two surfaces of the $BaTiO_3$ nanocube; the dashed line indicate the decrease of the piezoelectric polarization with a mechanical strain.

$BaTiO_3$ nanocube is under ultrasonic irradiation in water, both the periodic acoustic pressure of ultrasonic wave and the extreme pressure formed by the collapse of the acoustic cavitation walls can affect the intensity of the spontaneous electric potential in the $BaTiO_3$ nanocubes. It is known that under intensive ultrasound irradiation, water generates extremely active bubbles, which subsequently collapse and cause high local pressure (>100 MPa).[66] On the basis of our simulation (in Supporting Information S2), this high compressive stress can induce a piezoelectric potential around 0.36 V. Thus, a periodical absorption and release process of free charge in water occurs on the surface of $BaTiO_3$ nanocubes. Some metal-oxide−semiconductor nanostructures can function as good electrochemical catalysis electrodes.[67,68] The insulated surface of $BaTiO_3$ has no electrochemical catalytic activity but can act as voltage supplier. Thus, the Ag_2O−$BaTiO_3$ hybrid photocatalyst can exhibit sonocatalytic activity similar as an electrochemical catalytic process (Supporting Information S12). There is no doubt that ultrasonic driven piezoelectric effect of ferroelectric $BaTiO_3$ nanocubes can induce the release of free charge carriers into reaction system,[61,62] which reacts with organic pollutant through semiconductor Ag_2O and acts as a microelectrochemical reactor, and realize the electrochemical catalysis. However, the degradation efficiency of Rh B via sonocatalysis is very limited.

The photodegradation of Rh B with all the samples as catalysts was assessed under UV light irradiation without ultrasonic irradiation (Figure 2b) to evaluate the UV light photocatalytic activity of the samples. P25 possesses the best UV photocatalytic activity, and $BaTiO_3$ nanocubes do not possess any UV photocatalytic activity. Ag_2O has stronger photodegradation activity during an initial 2 h photocatalysis process compared with P25 but fails to approach a complete degradation of Rh B. The high UV photocatalytic activity of Ag_2O originates from the scarification reaction of Ag_2O nanoparticles during photocatalysis.[65] A large amount of elemental Ag can be detected after a 2 h photocatalysis, which demonstrates that the reduction of Ag_2O to Ag plays an important role in the efficient charge carrier separation (Supporting Information S13). However, unlike pure Ag_2O, the photocatalytic activity of Ag_2O−$BaTiO_3$ hybrid nanocubes retains after 2 h, although the degradation rate is slightly lower than that of the Ag_2O nanoparticles in the first 2 h. When Ag_2O was physically mixed with $BaTiO_3$, its UV photocatalytic activity became smaller than that of Ag_2O alone. It should be caused by the light-shield effect of individual $BaTiO_3$ nanocubes that possess no photocatalytic activity. When both UV light and ultrasonic irradiation are applied on the catalysis system, which is called as sonophotocatalysis, the Rh B degradation ability of P25, Ag_2O, and the Ag_2O−$BaTiO_3$ physical mixture is almost the same as that in the photocatalytic system under UV light irradiation only (Figure 2c and d). More than expected, for Ag_2O−$BaTiO_3$ hybrid nanocubes, Rh B can be totally degraded under both UV light and ultrasonic irradiation only in 1.5 h, which is dramatically short than that under UV light irradiation only (over 3 h), and even better than that with P25 as UV light photocatalyst (2.5 h).

The assistant of ultrasonic in a catalytic process is easier assigned to the improvement of transporting the reactants and products, as well as the improvement of radicals' generation.[48,49,52−54,56,57,69] However, as shown in Figure 2b and c, the Rh B degradation rates with Ag_2O as catalyst without and with ultrasonic are similar, whereas the ones with $BaTiO_3$ forming the heterostructure show a significant improvement. It implies that ultrasonic hardly works for the enhancement of Rh B degradation directly, and the media $BaTiO_3$ plays an important role.

Under photon excitation, electron and hole pairs are generated in an Ag_2O nanoparticle, but a random motion of the carriers results in a high recombination rate between the electrons and holes, reducing its function as catalyst (Figure 3a). In the Ag_2O−$BaTiO_3$ hybrid nanocubes, an electric field is created inside a $BaTiO_3$ nanocube along its spontaneous polarization direction, as indicated in Figure 3b (solid line).[70,71]

DOI: 10.1021/nl504630j
Nano Lett. XXXX, XXX, XXX−XXX

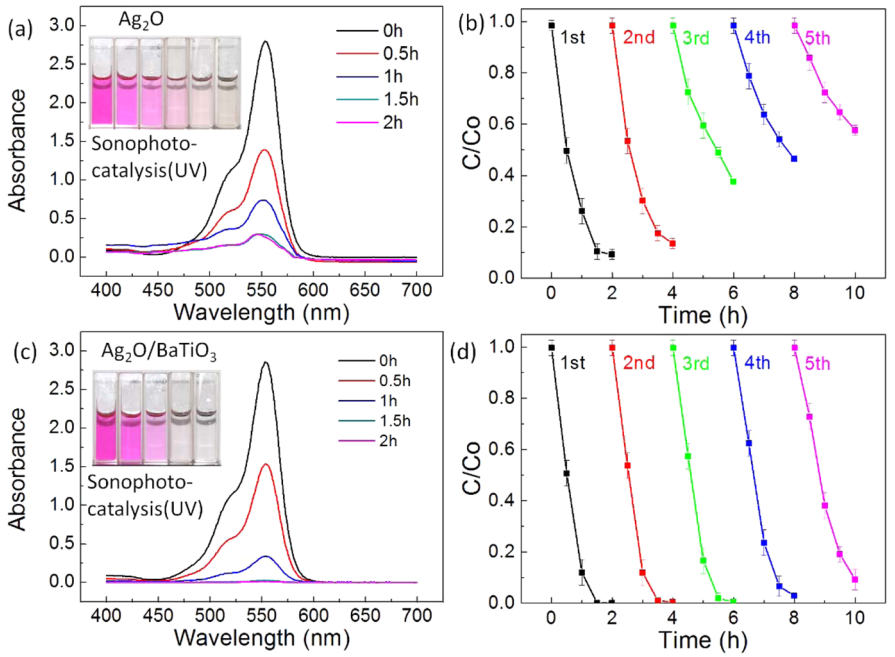

Figure 4. Absorption spectra of Rh B solution with different sonophotocatalysts under UV−ultrasonic irradiation treatment in the presence of Ag_2O (a) and Ag_2O−$BaTiO_3$ hybrid nanocubes (c), and their cyclic degradation curve (b) and (d), correspondingly.

This polar charge-created field is a driving force for attracting the holes in the Ag_2O nanoparticles attached to the left-hand surface to move toward the C− side of the $BaTiO_3$ cube (with negative polarization charges), while the electrons are being repelled to the surface of the nanoparticle. On the other side, electrons in the Ag_2O nanoparticle attached at the right-hand side of the $BaTiO_3$ nanocube are attracted to move toward the C+ side of the nanocube, while the holes are repelled toward the surface of the Ag_2O nanoparticle. The separation of photoinduced charge carriers with opposite signs in the two Ag_2O nanoparticles at the two surfaces of the $BaTiO_3$ nanocube, respectively, along the spontaneous polarized direction is the core of the improved photocatalysis.[2] However, for a static ferroelectric potential, this process continues until all of the piezoelectric polarization charges are fully screened by the free carriers. In our approach, the built-in field in Ag_2O−$BaTiO_3$ hybrid nanocubes was altered by applying a periodic stress on the $BaTiO_3$ nanocube as provided by the ultrasonic wave. When the $BaTiO_3$ nanocrystal is applied with compression stress induced by the ultrasonic wave, the polarization potential is diminished ($P_1 < P_0$). It implies the diminishing of the built-in field that would release most of the photoinduced electrons and holes attached on the C+ and C− surfaces of $BaTiO_3$ nanocubes abruptly (Figure 3, dash line). It is a fast discharge process for the $BaTiO_3$ nanocubes (Figure S15 in Supporting Information S12). Inversely, when the $BaTiO_3$ nanocube is free of strain, more photoinduced charge carriers will move toward the C+ and C− surfaces of $BaTiO_3$ nanocubes, which is a recharge process for the $BaTiO_3$ nanocubes. So, the piezoelectric charges will not be fully screened, due to the varying piezoelectric field, in responding to the excitation of the ultrasonic wave. As a result, the Ag_2O−$BaTiO_3$ hybrid nanocubes can remain active for photodegradation as long as both light and ultrasonic irradiation are supplied.

The results indicate that the alternative enlargement and diminishing of the built-in electric field induced by ultrasonic wave through the piezoelectric effect of $BaTiO_3$ is the key to enhance the photoelectric conversion process of photocatalytic semiconductor, which is known as the piezophototronic effect.[35,36,38,42,72] As reported, the small potential around 1.5 mV can induce around 5.6% enhancement of the piezoelectric photocurrent.[73] The piezoelectric polarized electric field (0.36 V, Supporting Information S2) induced by ultrasonic wave promotes the mobility of carriers, leading an efficient separation of the electron−hole pairs in photoelectric conversion process of piezoelectric-semiconductor hybrid materials. The low efficiency of degrading Rh B with a physically mixed Ag_2O and $BaTiO_3$ is attributed to the failure of the formation heterostructure between Ag_2O and $BaTiO_3$, which results in poor effectiveness of the electron−hole separation.

More experiments were performed to confirm the ultrasonic irradiation enhancement of the photocatalytic property of Ag_2O−$BaTiO_3$ hybrid nanocubes based on the piezophototronic effect.[34−38,42,72] First, the degradation property of Rh B was assessed under visible light, ultrasonic irradiation, and both visible light and ultrasonic irradiation by using the aforementioned five samples, P25, $BaTiO_3$ nanocubes, Ag_2O nanoparticles, a physical mixture of Ag_2O and $BaTiO_3$ nanocubes, and Ag_2O−$BaTiO_3$ hybrid nanocubes, as catalysts to check if Ag_2O−$BaTiO_3$ hybrid nanocubes also possess sonophotocatalytic properties under visible light irradiation (Supporting Information S14). For Ag_2O−$BaTiO_3$ hybrid photocatalyst, it takes 4 and 2.5 h to degrade Rh B completely without and with ultrasonic irradiation under visible light irradiation, respectively (Figure S18 in Supporting Information S14), which strongly supports the conclusion that the ultrasonic irradiation can enhance of the photocatalytic activity of Ag_2O−$BaTiO_3$ hybrid nanocubes based on the piezophototronic effect. The second experiment is to repeat the above experiments by using another important model organic pollutant, methyl orange (MO). The degradation rate of MO with Ag_2O−$BaTiO_3$ hybrid nanocubes under both light and ultrasonic irradiation is around 20% higher than that of the

DOI: 10.1021/nl504630j
Nano Lett. XXXX, XXX, XXX−XXX

other conditions (Figure S20 in Supporting Information S14). The third experiment is assessing sonophotocatalytic activity of $Ag_2O-BaTiO_3$ hybrid nanocubes under different ultrasonic frequency. In this study, ultrasonic transducers with different frequencies (20, 27, 40, 50, 60, 68, and 80 kHz) were selected as the ultrasonic sources (Supporting Information S15) to check the relation between the enhancement effect of the photocatalytic activity of $Ag_2O-BaTiO_3$ hybrid nanocubes and the ultrasonic frequency. The results indicate that the sonophotocatalytic activity of the $Ag_2O-BaTiO_3$ hybrid nanocubes relies on the ultrasonic frequency, and 27 kHz is the most effective frequency for the high performance of sonophotocatalysis. Moreover, the fourth experiment was done to clarify sonophotocatalysis strategy is universal. In this experiment, another very important ferroelectric material ($PbTiO_3$) was used as a built-in field source to repeat the experiment as $Ag_2O-BaTiO_3$ hybrid nanocubes (Supporting Information S16). The sonophotocatalytic activity of the $Ag_2O-PbTiO_3$ hybrid nanoparticles is much higher than that of the $Ag_2O-BaTiO_3$ hybrid nanoparticles. The complete sonophotocatalytic degradation time of Rh B decreases from over 3.5 to 1.5 h compared with that only under visible light irradiation. The reason should be attributed that the piezoelectric constant of $PbTiO_3$ is much higher than $BaTiO_3$. These results not only proved the universality of piezophototronic effect enhancement on ferroelectric-semiconductor sonophotocatalysts but also points that higher piezoelectric property of ferroelectrics can induce higher sonophotocatalytic activity.

To verify the degradation of Rh B is a mineralization process during the sonophotocatalysis with the Ag_2O catalyst and $Ag_2O-BaTiO_3$ hybrid catalyst, a series of UV−visible absorption spectra of the Rh B solution were recorded at different sonophotocatalysis times under UV light−ultrasonic irradiation. The results (Figure 4a and c) show that the intensity of all the Rh B peaks decrease with the treatment time increase without any new peaks appearing. It indicates that both catalysts can directly mineralize Rh B without any byproducts (Supporting Information S17). For Ag_2O, the sonophotocatalytic degradation rate of Rh B is only 90% in 2 h under UV light−ultrasonic irradiation (Figure 4a). However, for the $Ag_2O-BaTiO_3$ hybrid photocatalyst, the sonophotocatalytic degradation rate can reach 100% under UV light−ultrasonic irradiation in 2 h (Figure 4c). Another important discovery in this work is that the built-in field in the $Ag_2O-BaTiO_3$ hybrid nanocubes can improve the cyclic sonophotocatalytic property. The stability of sonophotocatalysis for the Ag_2O nanoparticles and $Ag_2O-BaTiO_3$ hybrid nanocubes was evaluated by checking their cyclic property. For Ag_2O nanoparticles, the sonophotocatalytic degradation rate decreases about 50% after five cycles under UV light−ultrasonic irradiation (Figure 4b), which indicates that the photoinduced electrons is not only used to degrade organic molecules but also consumed for reducing Ag_2O to elemental silver, thus decreasing the photocatalytic activity of the catalyst.[65] Surprisingly, the sonophotocatalytic cyclic ability of $Ag_2O-BaTiO_3$ hybrid nanocubes is dramatically improved under UV light−ultrasonic irradiation. After five cycles of sonophotocatalysis, there is less than a 10% decrease in the sonophotocatalytic activity (Figure 4d), which supports our suggestion that alternative enlargement and diminishing of the built-in electric field can maintain photoinduced carrier separation and even prohibit the electrons to react with Ag^+ from forming elemental silver. The experimental results on this section demonstrates that piezophototronic effect of $Ag_2O-BaTiO_3$ can not only enhance the photocatalytic activity but also endow a well cyclic property to $Ag_2O-BaTiO_3$ hybrid nanocubes. Piezophototronic effect is the key for getting high photocatalytic performance of $Ag_2O-BaTiO_3$ hybrid nanocubes.

In summary, the built-in electric field originated from the spontaneous polarization potential of ferroelectric nanocrystal can be used to enhance the photocatalytic activity of semiconductor photocatalysts through the enhancement of photoinduced charge carrier separation based on the built-in filed-induced periodical absorption and release process of the carriers. On the basis of stress-induced spontaneous polarization potential alternately variation of ferroelectrics and photocatalytic activity of semiconductor photocatalyst, sonophotocatalysis was suggested as a way of introducing a noncontact energy-supplying source to obtain continuous enhancement of the photocatalytic activity of semiconductor photocatalyst attached on the surface of ferroelectric nanocrystal. Under periodic ultrasonic pressure driving, the built-in field of a ferroelectric nanocrystal can be alternately altered by piezoelectric effect of ferroelectrics, which can induce, momentarily absorb, and suddenly release some photoinduced carriers and avoid saturating the built-in field. During sonophotocatalysis, the piezophototronic effect is the key for obtaining high photocatalytic performance of semiconductor/ferroelectrics hybrid sonophotocatalyst. In this paper, $Ag_2O-BaTiO_3$ hybrid nanocubes synthesized by assembling Ag_2O nanoparticles on $BaTiO_3$ nanocubes were used as a model sonophotocatalyst and responded favorably to ultrasonic irradiation as an effective sonophotocatalyst. Ferroelectric based hybrid photocatalyst and sonophotocatalysis will provide a new strategy for high performance photocatalysis applications.

■ ASSOCIATED CONTENT

Ⓢ Supporting Information

Additional information and figures, including experimental details, piezoelectric responses of $BaTiO_3$ nanocube and control experiments. This material is available free of charge via the Internet at http://pubs.acs.org.

■ AUTHOR INFORMATION

Corresponding Authors

*E-mail: hongliu@sdu.edu.cn.

*E-mail: zlwang@gatech.edu.

Author Contributions

⊥These authors contribute equal to this work.

Author Contributions

Hong Liu initiated, designed, and supervised the project. Zhong Lin Wang provided the theoretical framework and supervised the theoretical investigation part. Haidong Li and Yuanhua Sang designed and carried out the experiments, as well as the manuscript preparation. Sujie Chang and Huaidong Jiang assisted with the experiments. Xin Huang, Yan Zhang, and Rusen Yang carried out the numerical simulations.

Notes

The authors declare no competing financial interest.

■ ACKNOWLEDGMENTS

The authors would like to thank Prof. Robert I. Boughton from Bowling Green State University at Bowling Green for his professional suggestions, and the funding from the National Natural Science Foundation of China (Grant No. 51372142,

DOI: 10.1021/nl504630j
Nano Lett. XXXX, XXX, XXX−XXX

31430031, U1332118), the NSFC Innovation Research Group (IRG: 51321091) and the "100 Talents Program" of the Chinese Academy of Sciences. Thanks for the support from the "Thousands Talents" program for the pioneer researcher and his innovation team in China.

REFERENCES

(1) Cui, Y.; Briscoe, J.; Dunn, S. *Chem. Mater.* **2013**, *25* (21), 4215–23.
(2) Li, L.; Salvador, P. A.; Rohrer, G. S. *Nanoscale* **2014**, *6* (1), 24–42.
(3) Kim, C. O.; Kim, S.; Shin, D. H.; Kang, S. S.; Kim, J. M.; Jang, C. W.; Joo, S. S.; Lee, J. S.; Kim, J. H.; Choi, S. H.; Hwang, E. *Nat. Commun.* **2014**, *5*, 3249.
(4) Tian, J.; Zhao, Z.; Kumar, A.; Boughton, R. I.; Liu, H. *Chem. Soc. Rev.* **2014**, *43*, 6920–37.
(5) Paramasivam, I.; Jha, H.; Liu, N.; Schmuki, P. *Small* **2012**, *8* (20), 3073–103.
(6) Chen, X.; Liu, L.; Yu, P. Y.; Mao, S. S. *Science* **2011**, *331* (6018), 746–50.
(7) Li, L.; Rohrer, G. S.; Salvador, P. A.; Dickey, E. *J. Am. Ceram. Soc.* **2012**, *95* (4), 1414–20.
(8) Wadhwa, P.; Liu, B.; McCarthy, M. A.; Wu, Z.; Rinzler, A. G. *Nano Lett.* **2010**, *10* (12), 5001–5.
(9) Hu, Y.; Gao, J. *J. Am. Chem. Soc.* **2011**, *133* (7), 2227–31.
(10) Mao, Z.; Song, W.; Chen, L.; Ji, W.; Xue, X.; Ruan, W.; Li, Z.; Mao, H.; Ma, S.; Lombardi, J. R.; Zhao, B. *J. Phys. Chem. C* **2011**, *115* (37), 18378–83.
(11) Jung, Y.; Li, X.; Rajan, N. K.; Taylor, A. D.; Reed, M. A. *Nano Lett.* **2013**, *13* (1), 95–9.
(12) Suyatin, D. B.; Jain, V.; Nebol'sin, V. A.; Tragardh, J.; Messing, M. E.; Wagner, J. B.; Persson, O.; Timm, R.; Mikkelsen, A.; Maximov, I.; Samuelson, L.; Pettersson, H. *Nat. Commun.* **2014**, *5*, 3221.
(13) Mongin, D.; Shaviv, E.; Maioli, P.; Crut, A.; Uri Banin, N. D. F.; Vallee, F. *ACS Nano* **2012**, *6* (8), 7034–43.
(14) Zhou, H.; Qu, Y.; Zeid, T.; Duan, X. *Energy Environ. Sci.* **2012**, *5* (5), 6732–43.
(15) Li, R.; Zhang, F.; Wang, D.; Yang, J.; Li, M.; Zhu, J.; Zhou, X.; Han, H.; Li, C. *Nat. Commun.* **2013**, *4*, 1432.
(16) Bian, Z.; Tachikawa, T.; Zhang, P.; Fujitsuka, M.; Majima, T. *Nat. Commun.* **2014**, *5*, 3038.
(17) Pile, D. *Nat. Photonics* **2012**, *6* (10), 637.
(18) Lin, J.; Shen, J.; Wang, R.; Cui, J.; Zhou, W.; Hu, P.; Liu, D.; Liu, H.; Wang, J.; Boughton, R. I.; Yue, Y. *J. Mater. Chem.* **2011**, *21* (13), 5106.
(19) Pan, J.; Liu, G.; Lu, G. Q.; Cheng, H. M. *Angew. Chem.* **2011**, *50* (9), 2133–7.
(20) Giocondi, J. L.; Rohrer, G. S. *J. Am. Ceram. Soc.* **2002**, *86* (7), 1182–89.
(21) Wang, X.; Xu, Q.; Li, M.; Shen, S.; Wang, X.; Wang, Y.; Feng, Z.; Shi, J.; Han, H.; Li, C. *Angew. Chem.* **2012**, *51* (52), 13089–92.
(22) Xia, T.; Zhang, W.; Murowchick, J.; Liu, G.; Chen, X. *Nano Lett.* **2013**, *13* (11), 5289–96.
(23) Wen, Z.; Li, C.; Wu, D.; Li, A.; Ming, N. *Nat. Mater.* **2013**, *12* (7), 617–21.
(24) Giocondi, J. L.; Rohrer, G. S. *Top. Catal.* **2008**, *49* (1–2), 18–23.
(25) Tiwari, D.; Dunn, S. *J. Mater. Sci.* **2009**, *44* (19), 5063–79.
(26) Yuan, Y.; Reece, T. J.; Sharma, P.; Poddar, S.; Ducharme, S.; Gruverman, A.; Yang, Y.; Huang, J. *Nat. Mater.* **2011**, *10* (4), 296–302.
(27) Nayak, S.; Sahoo, B.; Chakia, T. K.; Khastgir, D. *RSC Adv.* **2014**, *4*, 1212–24.
(28) Varghese, J.; Whatmore, R. W.; Holmes, J. D. *J. Mater. Chem. C* **2013**, *1* (15), 2618.
(29) Park, K. I.; Xu, S.; Liu, Y.; Hwang, G. T.; Kang, S. J.; Wang, Z. L.; Lee, K. J. *Nano Lett.* **2010**, *10* (12), 4939–43.
(30) Wada, S.; Yano, M.; Suzuki, T.; Noma, T. *J. Mater. Sci.* **2000**, *35* (15), 3889–02.
(31) Berlincourt, D.; Jaffe, H. *Phys. Rev.* **1958**, *111* (1), 143–8.
(32) Oxbrow, C. F. *Nature* **1954**, *174*, 1091–93.
(33) Yang, J.; Chen, J.; Liu, Y.; Yang, W.; Su, Y.; Wang, Z. L. *ACS Nano* **2014**, *8* (3), 2649–57.
(34) Liu, Y.; Niu, S.; Yang, Q.; Klein, B. D. B.; Zhou, Y. S.; Wang, Z. L. *Adv. Mater.* **2014**, *26* (42), 7209–16.
(35) Wu, W.; Pan, C.; Zhang, Y.; Wen, X.; Wang, Z. L. *Nano Today* **2013**, *8* (6), 619–642.
(36) Wang, Z. L. *Adv. Mater.* **2012**, *24* (34), 4632–46.
(37) Wang, Z. L. Piezotronics and Piezophototronics. In *Device Research Conference (DRC), 2012 70th Annual*; IEEE: Piscataway, NJ, 2012; pp 23–24.
(38) Wang, Z. L. *Nano Today* **2010**, *5* (6), 540–52.
(39) Wang, Z. L. *Adv. Mater.* **2007**, *19* (6), 889–92.
(40) Wang, X.; Song, J.; Liu, J.; Wang, Z. L. *Science* **2007**, *316* (5821), 102–5.
(41) Wang, Z. L.; Song, J. *Science* **2006**, *312* (5771), 242–6.
(42) Hu, Y.; Chang, Y.; Fei, P.; Snyder, R. L.; Wang, Z. L. *ACS Nano* **2010**, *4* (2), 1234–40.
(43) Mahvi, A. *Iran. J. Public Health* **2009**, *38* (2), 1–17.
(44) Terasaki, N.; Yamada, H.; Xu, C.-N. *Catal. Today* **2013**, *201*, 203–8.
(45) Wang, J.; Guo, B.; Zhang, X.; Zhang, Z.; Han, J.; Wu, J. *Ultrason. Sonochem.* **2005**, *12* (5), 331–7.
(46) Shimizu, N.; Ogino, C.; Dadjour, M. F.; Murata, T. *Ultrason. Sonochem.* **2007**, *14* (2), 184–90.
(47) Ertugay, N.; Acar, F. N. *Desalin. Water Treat.* **2013**, *51* (40–42), 7570–76.
(48) Gao, J.; Jiang, R.; Wang, J.; Wang, B.; Li, K.; Kang, P.; Li, Y.; Zhang, X. *Chem. Eng. J.* **2011**, *168* (3), 1041–8.
(49) Berberidou, C.; Poulios, I.; Xekoukoulotakis, N. P.; Mantzavinos, D. *Appl. Catal., B* **2007** 2007, *74*, (1–2), 63–72.
(50) Zhai, Y.; Li, Y.; Wang, J.; Wang, J.; Yin, L.; Kong, Y.; Han, G.; Fan, P. *J. Mol. Catal. A: Chem.* **2013**, *366*, 282–7.
(51) Ince, N. H.; Tezcanli, G.; Belen, R. K.; Apikyan, I. G. *Appl. Catal., B* **2001**, *29* (3), 167–76.
(52) Kritikos, D. E.; Xekoukoulotakis, N. P.; Psillakis, E.; Mantzavinos, D. *Water Res.* **2007**, *41* (10), 2236–46.
(53) Selli, E. *Phys. Chem. Chem. Phys.* **2002**, *4* (24), 6123–8.
(54) Wang, Y.; Zhao, D.; Ma, W.; Chen, C.; Zhao, J. *Environ. Sci. Technol.* **2008**, *42* (16), 6173–78.
(55) Wang, J.; Zhou, S.; Wang, J.; Li, S.; Gao, J.; Wang, B.; Fan, P. *Ultrason. Sonochem.* **2014**, *21* (1), 84–92.
(56) Gonzalez, A. S.; Martinez, S. S. *Ultrason. Sonochem.* **2008**, *15* (6), 1038–42.
(57) Vinu, R.; Madars, G. *Environ. Sci. Technol.* **2009**, *43* (2), 473–9.
(58) Joseph, C. G.; Puma, G. L.; Bono, A.; Taufiq-Yap, Y. H.; Krishnaiah, D. *Desalination* **2011**, *276* (1–3), 303–9.
(59) Joseph, C. G.; Li Puma, G.; Bono, A.; Krishnaiah, D. *Ultrason. Sonochem.* **2009**, *16* (5), 583–9.
(60) Joseph, C. G.; Liew, Y. L. S.; Krishnaiah, D.; Bono, A. *J. Applied Sci.* **2012**, *12* (18), 1966–71.
(61) Hong, K.-S.; Xu, H.; Konishi, H.; Li, X. *J. Phys. Chem. Lett.* **2010**, *1* (6), 997–1002.
(62) Hong, K.-S.; Xu, H.; Konishi, H.; Li, X. *J. Phys. Chem. C* **2012**, *116* (24), 13045–51.
(63) Smith, M. B.; Page, K.; Siegrist, T.; Redmond, P. L.; Walter, E. C.; Seshadri, R.; Brus, L. E.; Steigerwald, M. L. *J. Am. Chem. Soc.* **2008**, *130* (22), 6955–63.
(64) Tjeng, L.; Meinders, M.; van Elp, J.; Ghijsen, J.; Sawatzky, G.; Johnson, R. *Phys. Rev. B* **1990**, *41* (5), 3190–9.
(65) Zhou, W. J.; Liu, H.; Wang, J.; Liu, D.; Du, G.; Cui, J. *ACS Appl. Mater. Interfaces* **2010**, *2* (8), 2385–92.
(66) Flint, E. B.; Suslick, K. S. *Science* **1991**, *253* (5026), 1397–9.
(67) Lewerenz, H. J.; Heine, C.; Skorupska, K.; Szabo, N.; Hannappel, T.; Vo-Dinh, T.; Campbell, S. A.; Klemm, H. W.; Munoz, A. G. *Energy Environ. Sci.* **2010**, *3* (6), 748–60.

DOI: 10.1021/nl504630j
Nano Lett. XXXX, XXX, XXX–XXX

(68) Yang, J.; Wang, D.; Han, H.; LI, C. *Acc. Chem. Res.* **2013**, *46* (8), 1900−9.
(69) Kaur, S.; Singh, V. *Ultrason. Sonochem.* **2007**, *14* (5), 531−7.
(70) Yaacobi-Gross, N.; Soreni-Harari, M.; Zimin, M.; Kababya, S.; Schmidt, A.; Tessler, N. *Nat. Mater.* **2011**, *10* (12), 974−9.
(71) Singh-Bhalla, G.; Bell, C.; Ravichandran, J.; Siemons, W.; Hikita, Y.; Salahuddin, S.; Hebard, A. F.; Hwang, H. Y.; Ramesh, R. *Nat. Phys.* **2010**, *7* (1), 80−6.
(72) Wang, Z. L.; Wu, W. *Natl. Sci. Rev.* **2014**, *1* (1), 62−90.
(73) Shi, J.; Starr, M. B.; Xiang, H.; Hara, Y.; Anderson, M. A.; Seo, J. H.; Ma, Z.; Wang, X. *Nano Lett.* **2011**, *11* (12), 5587−93.

DOI: 10.1021/nl504630j
Nano Lett. XXXX, XXX, XXX−XXX